Available online at www.sciencedirect.com

ScienceDirect

Physics Procedia 56 (2014) 48 – 57

Physics Procedia

8th International Conference on Photonic Technologies LANE 2014

Experimental approbation of selective laser melting of powders by the use of non-Gaussian power density distributions

Anna Okunkova[a,]*, Marina Volosova[a], Pavel Peretyagin[a], Yuri Vladimirov[a], Ivan Zhirnov[a], A.V. Gusarov[a,b]

[a]*Moscow State University of Technology "STANKIN", Vadkovsky pereulok 3a, 127055 Moscow, Russian Federation*
[b]*École Nationale d'Ingénieurs de Saint-Étienne, 58 rue Jean Parot,42023 Saint-Etienne, France*

Abstract

Experimental results on laser beam modulation at selective laser melting (SLM) are presented. The modulation is a possible way to improve the efficiency of the SLM process. The optical diagnostics shows the energy loss up to 30%. This could be a consequence of high thermal gradients in the melt pool resulted by the Gaussian power density distribution. The Gaussian distribution can be changed to the flat-top one or to the inverse-Gaussian (donut) one. An experimental stand with a 200W laser source was developed. Twenty single tracks for each of the three modes were obtained for a Co-Cr alloy. The samples were studied by scanning electronic microscopy (SEM) on irregularity. Optical diagnostics by high velocity camera (HVC) shows that the use of the non-Gaussian laser beam distributions can significantly reduce the width of the free-of-powder consolidation zone, which is considered as the main reason for irregularity of single tracks. A better metallurgical bonding of the single tracks with the substrate was obtained by the use of the flat-top laser beam. Both of these facts show a significant influence of the laser beam energy distribution on the energy loss at SLM, especially for high power laser sources. The observed escape of granules shows a possible influence of the dynamic factor. The use of the non-Gaussian distributions can enhance 3D parts, for example, improve the geometrical tolerance and decrease the residual porosity.

Peer-review under responsibility of the Bayerisches Laserzentrum GmbH

Keywords: Additive manufacturing; selective laser melting; laser beam modulation; non-Gaussian power density distribution

* Corresponding author. Tel.: +7-909-913-1207 ; fax: +7-499-973-39-17 .
E-mail address:a.okunkova@stankin.ru, 9131207@gmail.com

Peer-review under responsibility of the Bayerisches Laserzentrum GmbH
doi:10.1016/j.phpro.2014.08.095

1. Introduction

The technology of selective laser melting (SLM) is one of the methods to build up 3D objects based on layer-by-layer principles. It's an alternative to the traditional methods of processing and manufacturing. SLM is actively used for different applications. For example, application of SLM for implants from bioglass and bioceramics is discussed by Esteban-Tejeda et al. (2012). Shishkovsky et al. (2013) argues that SLM is useful in the aerospace industry for fabrication parts from oxide ceramics and intermetallic alloys.

In the last few years, the possibility to improve the productivity by the increase of power of the laser source was studied. Up to now, it does not give clear results. The experiments and the optical diagnostics show the non-desirable effects as overheating of the melt pool, the powder granule escape, and the Marangoni flow (see Yadroitsev et al. (2010)).

One of the reasons of the non-desirable effects could be high temperature gradients in the melt pool. It makes the track less homogenized and significantly enlarges the width of the free-of-powder consolidation zone (Yadroitsev et al. (2013)). The droplets, which escape from the melt pool, can damage the optical system of the SLM machine and pollute the ambience. This effect influences the microstructure of the material and can considerably reduce the mechanical properties (Doubenskaya et al. (2012, 2013)). The escape of droplets is supposed to depend on the gradient of power density distribution in the laser spot on the powder layer, which creates high-speed melt flows in the processing zone (Gusarov et al. (2007), Smurov et al. (2012)). The flows influence the granules near the board of the melt pool and heat them up. These effects were described by mathematical models (Gusarov et al. (2013)).

Today the SLM machine builders have no solution on the industry level. The above non-desirable effects can be only reduced by smoothing the temperature gradients in the melt pool. There are two main ways to achieve it: the preheating of the powder layer and the modulation of the laser beam. The powders can be preheated by preheating the working platform. But it is difficult to realize because of the problem of the heating coil placement.

Meanwhile, there are much more opportunities for laser beam modulation. These opportunities have been studied by different scientists in the period of 2000-2012 (Hendrics et al. (2012), Dickey et al. (2006), Voelkel and Weible (2008), Voelkel et al. (2005)) as a principal possibility to change a laser beam mode from the Gaussian one to the flat-top and the donut ones. However, there are no appropriate experimental studies for the SLM process.

The approach could correct the gradient of temperatures in the melt pool (to make it more smooth and uniform) with the purpose to create optimal conditions of the heat and mass transfer which can reduce or completely exclude the non-desirable effects as the droplets escape. The proposed shaping of the laser beam could reduce the porosity and the cracking of the parts and improve their quality and geometrical tolerance.

Nomenclature

A	laser beam cross section area, mm^2
D	laser beam diameter, mm
f'	focus distance F-theta lens, mm
R	distance between different distributions, mm
λ	laser wave length, μm
P	laser power, W
V	laser scanning speed, mm/sec
W	single track width, μm
L	width of powder consolidation area, μm
E_S	specific energy, J/mm^2
E_d	specific energy density distribution, J/mm^3

2. Problem statement

Dickey et al. (2006) showed that obtaining a uniform temperature field in the heating zone is possible with the flat-top or even the inverse-Gaussian laser beam mode. Klocke et al. (2003) defined around twelve main parameters

of SLM related to the laser source, the base platform, the atmosphere, and the powder. All the parameters were graded as the input and output controlled technological parameters (Fig. 1).

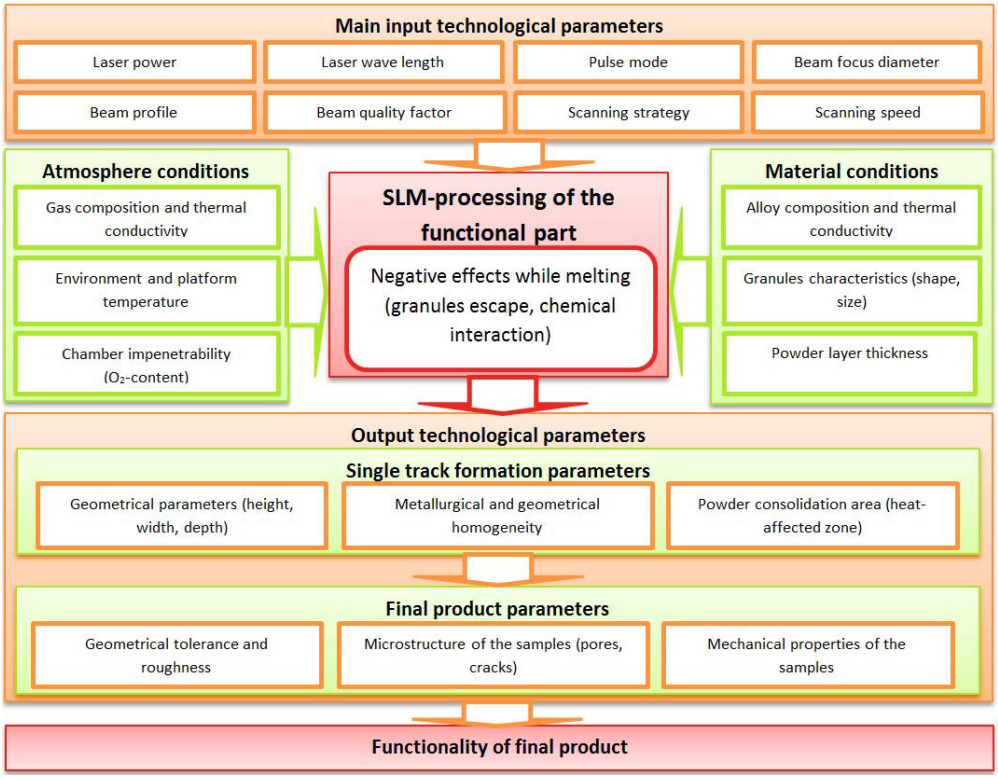

Fig. 1. Functional dependence for input and output parameters at SLM.

The following tasks have been formulated: to develop an experimental stand for selective laser melting of the powders including a system of laser beam modulation and a system of video monitoring; to establish on the system stable the Gaussian, the flat-top and the inverse-Gaussian laser beam mode; to investigate the working parameters of the system for each laser beam mode (for Co-Cr powder) with the purpose to obtain stable single tracks; to adapt a video monitoring system for studying the single track formation while processing for the negative effects as granules escape; to study the output parameters for the single tracks produced at different laser modes as the geometrical parameters and the homogeneity and the free-of-powder consolidation zone (heat-affected); to estimate the single track penetration depth and its metallurgical homogeneity in the cross-section.

3. Experimental work

3.1. Experimental stand and equipment

The experimental stand (Figs. 2, 3) has been developed. The laser source is the ytterbium fiber laser LK-200-V with the wavelength λ=1.07 μm. The collimated laser beam has the effective diameter of 5 mm after optical collimator 4. The laser beam goes through f-piShaper 5 and next through scanner 6, where afterwards achieves the working base platform and the powder by the movable optical mirrors and focus lens 7.

The profile of the laser beam is monitored by CCD-camera 13. Optical mirror BCube 11 and an optical attenuator have been used for reduction of the laser beam power on the objective of the camera. High-speed camera 9 (frame rate 775000 s^{-1}, maximum resolution 1,024 x 1,000 pixels) has been used to visualize the melting process.

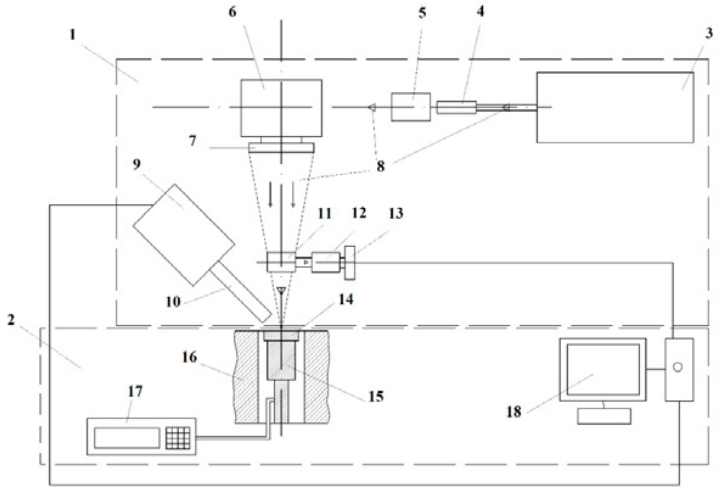

Fig. 2. Experimental stand principal scheme: 1 - optical part including 3-ytterbium fiber laser, 4 - optical collimator, 5 – pi-Shaper, 6 - scanning head, 7 - F-theta focusing lens, 8 - laser beam optical path, 9 - high-speed camera Photron SA5 10 - macro lens NAVITAR 6000, 11 - optical mirror BCube, 12 - optical attenuator 13 - CCD camera LaserCam-HRTM; and 2 - mechanical part including 14 - stainless steel substrate with Co-Cr powder layer, 15 - movable piston, 16 working platform, 17-micrometer, 18 - PC.

The mechanical part of the stand consists of the base platform 14 made of low-carbon stainless steel which is used as a basis for deposing the powder (diameter 45 mm and height 8 mm). The discrete step of the engine can be varied. The platform base is placed on working piston 15 of platform 16. The movement of piston is controlled by micrometer 17. The geometrical tolerance for the working surfaces was ± 0.02 mm.

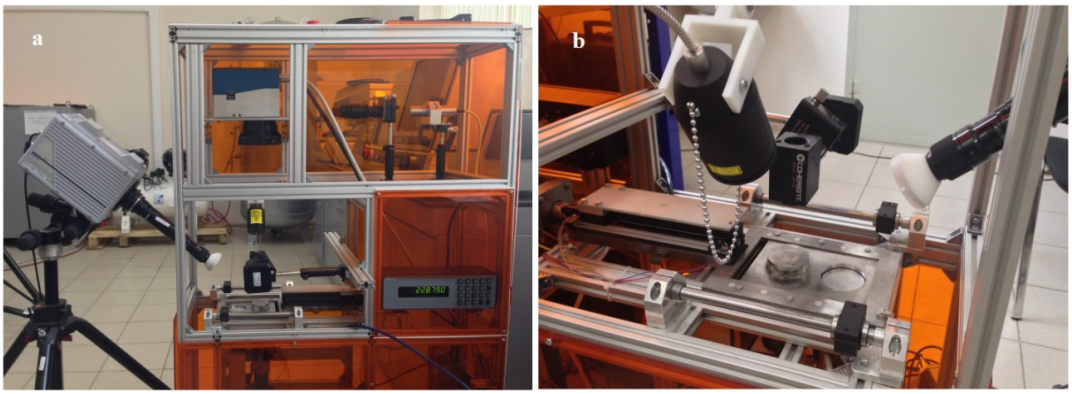

Fig. 3. Photo of the experimental stand: (a) general view; (b) working area.

Co-Cr powder was used in experiments (Co (60-65)%, Cr (26-30)%; Mo (5-7)%; Si and Mn less 1%, Fe less 0,75%, C less 0,16%, Ni less 0,10%). Protecting atmosphere was not used because there was no possibility to put all monitoring and optical equipment on the stand. According to the literature data, Co-Cr powder has a low reactivity with air in comparison with other powders (Ti6Al4V alloy, maraging steel etc.).

The powder layer thickness was measured by optical microscope Olympus BX51M. The cross-sections of single tracks were prepared by conventional methods using the technological complex ATM (consists of the cutting machine, the hydraulic press, and the polishing machine).

The structure of single tracks was studied by scanning electronic microscope VEGA 3 LMH (TESCAN) with the maximum magnification about 1M. The microscope is equipped with the secondary and backscattered electron detectors and EDX analysis of Oxford Instruments.

3.2. Experimental methods and techniques

In the experiments, a layer of powder is deposited on the working platform. The thickness of the each layer was monitored by the optical microscope. A micrometric screw was revolved on the table to control the thickness and the focus distance from the working base to the upper surface of the powder layer. The thickness was measured in three different points. The average thickness for the powder was 80 μm (±5 μm).

In accordance with the focus distance of F-theta lens of 420 mm, the working surface was placed at this distance to attain the maximum energy concentration on the powder surface. The placement of the working platform was fixed as the initial placement of the working surface. The laser beam mode and the effective diameter were detected by the CCD-camera (Fig. 4).

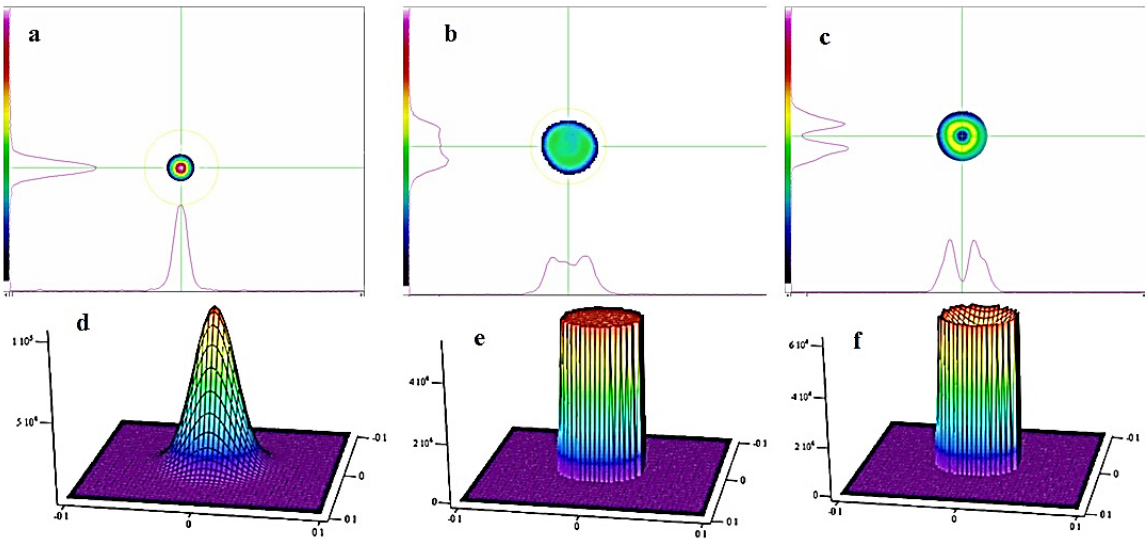

Fig. 4. Laser beam profile analysis by the CCD-camera: (a) Gaussian beam; (b) flat-top; and (c) inverse Gaussian power distribution.

In accordance with the special features of the experimental stand and for reduction of the error influence for the rotate ring on the optical tool as piShaper an optical system was fixed. Hence the changes of the power distribution were produced by distance changes from working surface to focus lens. The effective diameter of the laser beam (86.5%) was defined as 0.111 mm, the effective area was 0.261 mm^2.

For calculation of the distance between different distributions the next formula has been used:

$$R = \frac{8\lambda f'^2}{\pi D^2} \tag{1}$$

λ - laser wave length, f' - focus distance F-theta lens, D - laser beam diameter after collimator.

The working surface was moved in accordance with known distance between different distributions (20 mm). Extra two distributions were achieved by this method and have been controlled by CCD-camera: flat-top and inverse Gaussian (fig. 4 (b) and (c) accordingly).

Three main input parameters were considered for the experiments: the laser profile, the laser power and the scanning speed. The laser power was ranged from 15 to 180 W; the scanning speed was ranged from 2 to 120 mm/sec.

The single tracks was done on the powder-free base platform to corroborate an accordance for the optical distance between laser beam mode and working platform movements (working input parameters: P = 32 W, V = 15 mm/sec). There were produced five single tracks for each mode. The width of each single track was measured on the optical microscope and compared with the laser beam diameters received at CCD-camera.

The movements of the working surface (powder layer on the working platform) were produced for the experimentation work as following:

- As an absolute zero have been taken a working surface placement on the same level with working platform of experimental stand. The placement corresponds to the inverse Gaussian distribution (donut);
- The Gaussian (normal) distribution was achieved in the focus of F-theta lens, when the working platform was in position -15mm;
- The flat-top distribution was achieved in position -5 mm.

Table 1. Main input parameters for the experimental work.

N parameters group	1	2	3	4	5	6	7	8	9	10
Scanning speed (V), mm/sec	10	10	10	15	25	30	30	50	75	100
Laser power (P), W	30	50	70	50	50	30	50	100	150	50
Gaussian distribution	1	1	1	1	1	1	1	1	1	1
Flat-top distribution	1	1	1	1	0	1	1	1	0	1
Inverse Gaussian (Donut)	1	1	0	1	0	1	1	1	0	1

The effective diameter of the laser beam for the donut distribution was 0.347 mm and the effective area was 0.124 mm^2. The effective diameter of the laser beam for the flat-top distribution was 0.260 mm and the effective area was 0.165 mm^2. The experimental input parameters showed in the table 1.

All tracks have been video-recorded. Five single tracks were produced for each group of the input parameters (25 parameters group). The main groups, which demonstrate formation of single tracks, are represented in the table (1 – single track formation, 0 – no single track formation).

The high-velocity camera Photron SA5 was used for the visualization of the melting processes. The laser diode illumination with the 810 nm filter was used for excluding of the influence of the laser beam light and the thermal radiation. The parameters of the recording were selected to optimize detection of powder granules emission from the melt pool (frame rate and pulse frequency of illumination 1000 Hz, 1024x1024 points resolution, shutter 999 microseconds).

4. Results and discussion

Tracks with parameters listed in Table 1 were obtained. No track formation was observed at the scanning speed less than 10 mm/s or greater than 100 mm/s and the laser power less than 30 W or greater than 150 mm/s. The powder thickness was 80 μm. Some of the parameter groups showed stable results for single track formation at each laser beam mode (N1, 2, 4, 6, 7, and 8).

For two groups of stable parameters (N 4, 8), the average and the specific track width and the average and the specific widths of the free-of-powder consolidation zone were measured (Table 2). The specific width of a single track was defined as:

$$W_S = \frac{W_A - D}{2} \tag{2}$$

where W_A is the measured width of the single track and D the measured laser beam diameter. The specific width of the powder consolidation area was defined by a similar formula.

The significant reduction of the specific values for the width of the tracks and the free-of-powder consolidation zone is shown in Table 2.

Table 2. Average and specific track width and width of the free-of-powder consolidation zone for two input parameters groups.

Main input parameters	V = 15 mm/s, P = 50W (N4)				V = 50 mm/s, P = 100W (N8)			
Measured output geometrical parameters	W_A, µm	W_S, µm	L_A, µm	L_S, µm	W_A, µm	W_S, µm	L_A, µm	L_S, µm
Gaussian distribution	193,9	41,5	447,6	168,3	185,4	35,9	399,7	125,9
Flat-top distribution	170,8	-44,6	476,8	108,4	193,3	-35,3	384,1	73,2
Inverse Gaussian (donut)	170,8	-88,1	499,2	76,1	199,8	-73,2	435,7	41,2

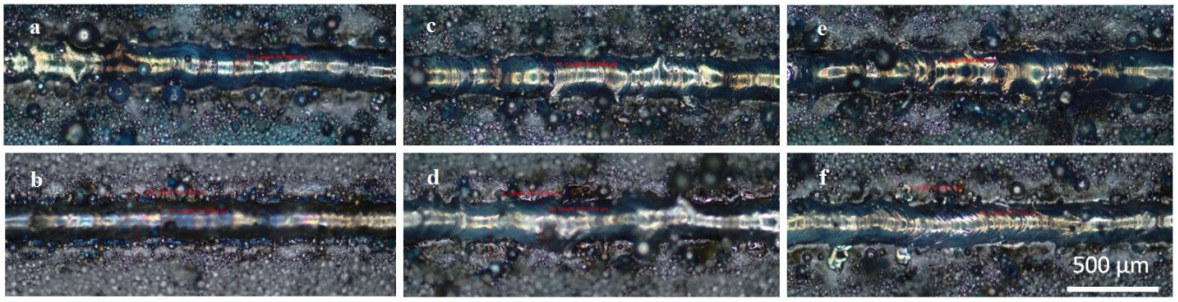

Fig. 5. Single track formation for different laser beam power distribution: Gaussian (a, b), flat-top (c, d) and donut (e, f); for two input parameters groups, N4 (a, c, e) and N8 (b, d, f).

The photos of the tracks obtained by optical microscopy show the stable track formation at SLM (Fig.5). The morphology of tracks of the parameters group N4 (a, c, e) indicates the non-desirable flows in the melting zone. These tracks probably consist of a suite of overlapped drops. This demonstrates the overheating effects in the melting zone. The increase of the scanning speed reduces the overheating effects at the same laser power.

The same effects can be seen in Fig. 5 (d, f). The increase of the scanning speed would be favorable for the represented input parameters and the laser beam profiles (flat-top and donut). The track in Fig. 5 (f) shows the feather-like character of the melt pool, which demonstrates a dynamic impact at single track formation.

The combined input parameters (the specific energy (3) and the specific energy density distribution (4)) were taken into account in the further work for the purpose to obtain stable input parameters for stable formation of single tracks. The images of the obtained tracks are shown in Fig. 6. The optical microscopy demonstrated that the specific energy gives better results. The stabilized input parameters were calculated according to Eq. (3) for single tracks formation at different laser beam profiles:

$$E_S = \frac{P}{DV} \tag{3}$$

$$E_d = \frac{4P}{\pi D^2 V} \tag{4}$$

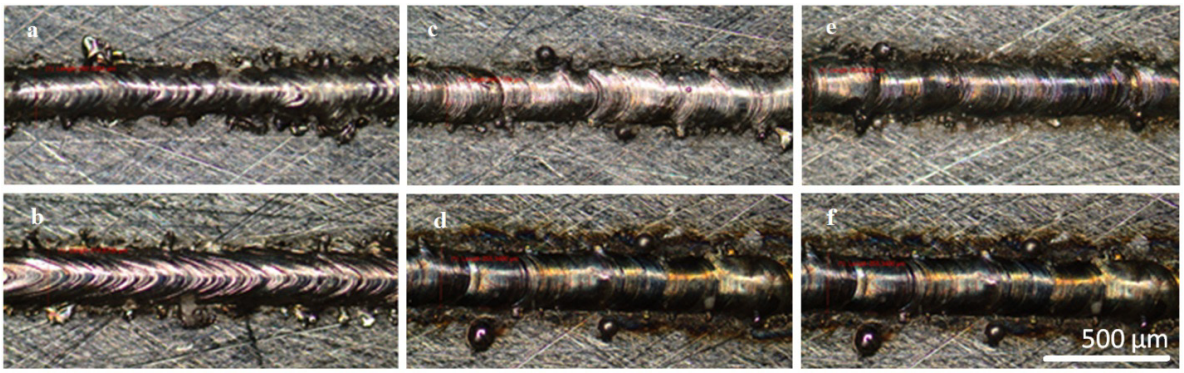

Fig. 6. Single track formation for different laser beam power distribution: Gaussian (a, b), flat-top (c, d) and donut (e, f); with the stabilized combined parameters obtained by calculation of the specific energy and the specific energy density distribution.

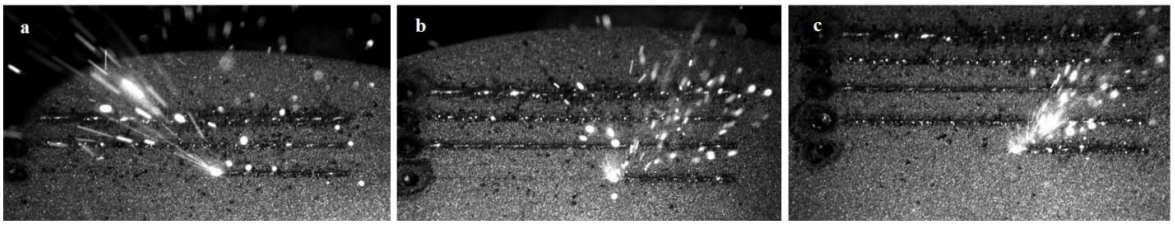

Fig. 7. Visualization of the single track formation for different laser beam power distributions: Gaussian (a), flat-top (b) and donut (c). Input parameters group N8.

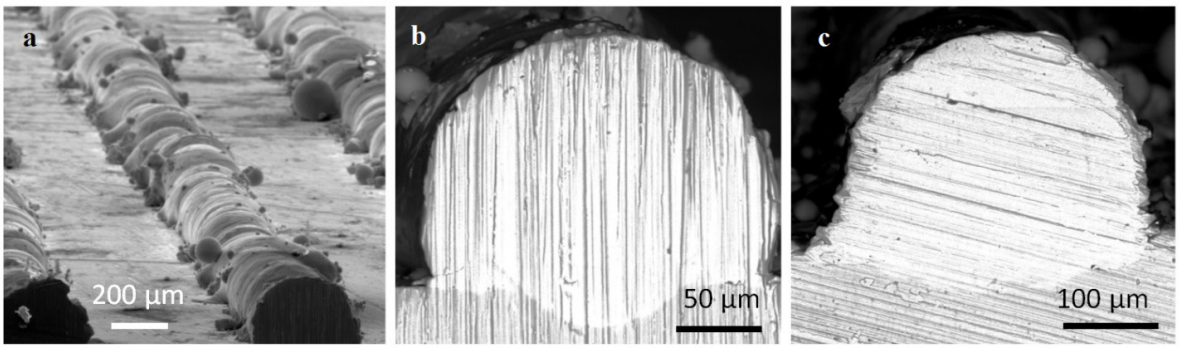

Fig. 8. SEM-analysis of the single tracks: (a) general view; (b) Gaussian and (c) flat-top. Input parameters group N4.

The video-visualization of the melting zone demonstrates very specific results (Fig. 7). The quantity of the emitted granules which leave the melt pool, and their velocity significantly reduce at the flat-top laser beam profile in comparison with the Gaussian one.

Fig. 7 (a) shows that the predominant direction of the granules emission is the same as the laser beam direction. The granules are also emitted all over around the melt pool. Meanwhile, Fig. 7 (b) shows that the granules do not emit all over around. The direction of the emission could be defined as vertical and orthogonal to the working platform. There are less emitted granules; their velocity and their spread are also less. The described effect of the flat-top laser beam profile can be considered as an advantage and could be recommended for industrial use after additional verification at a wider range of the input parameters (higher laser power and higher scanning speed).

Fig. 7 (c) shows the increase of the quantity of the emitted granules for the donut laser beam profile in comparison with the Gaussian and the flat-top ones. The velocity of the granules is less in comparison with the Gaussian profile, but greater in comparison with the flat-top laser beam. The direction of the escape is changed to the opposite. This effect is also proposed to be studied at a wider range of the input parameters. The effect of the direction changes for the emitted granules shows a dynamic impact which has to be studied in perspective.

Next the cross-section of the tracks were studied by scanning electronic microscopy. Fig. 8 shows more uniform remelting with the platform base for the flat-top beam. The Gaussian beam profile gives a deeper character of the remelted zone in the center of the single track. Strong metallurgical bonding was not observed for the donut laser distribution.

4. Conclusions

The main difference between the tracks was found at studying the free-of-powder consolidation zone. The width of this zone reduces when the distribution changes from the Gaussian one to the donut one. This change is favorable to improve the geometrical tolerance of 3D parts. As well, it indirectly shows the reduction of the non-desirable effects as the granules emission from the melt pool. The study shows that the non-Gaussian laser beam distributions significantly reduce the width of the free-of-powder consolidation zone, which is considered as the main reason for irregularity of single tracks.

The single track obtained by the Gaussian laser beam profile shows a deeper remelted zone in the center of the track than on its periphery. The flat-top laser beam profile shows more regular character for the melting zone, which demonstrates more homogenized metallurgical bonding.

Both of these facts show a significant influence of the laser beam energy distribution on the energy loss at selective laser melting, especially for high power laser sources.

Optical diagnostics by the high velocity camera (HVC) reveals that the direction of granules escape from the melt pool is changed from the forward one at the Gaussian profile to the backward one at the donut profile. The reason for this is not completely studied; however the influence of the dynamic factor is probable.

The use of the non-Gaussian distributions can enhance 3D parts, for example, improve the geometrical tolerance and decrease the residual porosity.

Acknowledgements

This work has been financed by the Ministry of Education and Science of the Russian Federation in the frames of the governmental task in the field of scientific activities.

References

Dickey, F.M., Holswade, S.C., Shealy, D.L. 2006. Laser Beam Shaping Application, Taylor and Francis Group, CRC Press.

Doubenskaia M., Pavlov M., Grigoriev S., Tikhonova E., Smurov I. 2012. Comprehensive Optical Monitoring of Selective Laser Melting. Journal of Laser Micro Nanoengineering 7, 3. 236-243.

Doubenskaia M., Pavlov M., Grigoriev S., Smurov I. 2013. Definition of brightness temperature and restoration of true temperature in laser cladding using infrared camera. Surface & Coatings Technology 220, 244-247.

Esteban-Tejeda L., Cabal B., Malpartida F., Lopez-Piriz R., Torrecillas R., Saiz E., Tomsia A.P., Moya J.S. 2012. Soda-lime glass-coating containing silver nanoparticles on Ti-6Al-4V alloy.Journal of the european ceramic society32, 11. 2723-2729.

Gusarov A.V., Yadroitsev I., Bertrand Ph., Smurov I. 2007.Heat transfer modelling and stability analysis of selective laser melting. Applied Surface Science, 254, 4, 975-979.

Gusarov A. V., Malakhova-Zjablova I. S., Perestoronina A. V. 2013. Calculation of Residual Stresses under Selective Laser Melting of Powders", Metallofizika I Noveishie Tekhnologii. 35, 11. P. 1501-1516.

Hendriks, A., Naidoo, D., Roux, F.S., López-Mariscal C., Forbes A. 2012.The generation of flat-top beams by complex amplitude modulation with a phase-only spatial light modulator, Proc. SPIE 8490.

Klocke F., WagnerC., AderC. 2003. Development of an integrated model for selective laser sintering. Proc. 36th CIRP International Seminar on Manufacturing Systems, June 03-05, 2003, Saarbrucken, Germany, 387-392.

Shishkovsky I.V., Yadroitsev I.A., Smurov I.Yu. 2013. Manufacturing three-dimensional nickel titanium articles using layer-by-layer laser-melting technology. Technical physics letters39, 12. 1081-1084.

Smurov I.Yu, Yadroitsev I.A., Movchan I.A., Okunkova A.A., Cherkasova N.Yu., Antonenkova G.V. 2012. Additive straight manufacturing by laser. Experimental work.Vestnik MSTU «STANKIN» 1, 1, 36-38.

Voelkel, R., Weible, K.J. 2008. Laser Beam Homogenizing: Limitations and Constraints, Proc. SPIE.

Voelkel, R., Eisner, M., Weible, K. J. 2005. Micro-optics: manufacturing and characterization, Proc. SPIE 5965.

Yadroitsev I., Gusarov A., Yadroitsava I., Smurov I. 2010.Single track formation in selective laser melting of metal powder. J. Mater. Processing Technology 210, 1624.

Yadroitsev I., Bertrand P., Antonenkova G., Grigoriev S., Smurov I. 2013. Use of track/layer morphology to develop functional parts by selective laser melting. Journal of Laser Applications 25, 5.